

## Symmetric Halogen Bonding Is Preferred in Solution

Anna-Carin C. Carlsson,<sup>†</sup> Jürgen Gräfenstein,<sup>†</sup> Adnan Budnjo,<sup>†,||</sup> Jesse L. Laurila,<sup>†,§</sup> Jonas Bergquist,<sup>‡</sup> Alavi Karim,<sup>†</sup> Roland Kleinmaier,<sup>†</sup> Ulrika Brath,<sup>†</sup> and Máté Erdélyi<sup>\*,†,#</sup>

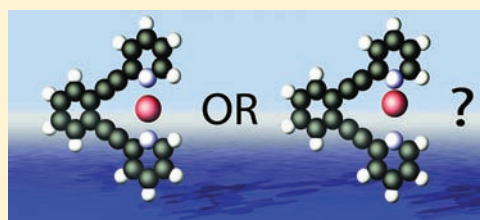
<sup>†</sup>Department of Chemistry and Molecular Biology, University of Gothenburg, SE-412 96 Gothenburg, Sweden

<sup>‡</sup>Analytical Chemistry, Department of Chemistry - Biomedical Center, Uppsala University, SE-751 24, Uppsala, Sweden

<sup>#</sup>The Swedish NMR Centre, Medicinargatan 5c, SE-413 90 Gothenburg, Sweden

### Supporting Information

**ABSTRACT:** Halogen bonding is a recently rediscovered secondary interaction that shows potential to become a complementary molecular tool to hydrogen bonding in rational drug design and in material sciences. Whereas hydrogen bond symmetry has been the subject of systematic studies for decades, the understanding of the analogous three-center halogen bonds is yet in its infancy. The isotopic perturbation of equilibrium (IPE) technique with <sup>13</sup>C NMR detection was applied to regioselectively deuterated pyridine complexes to investigate the symmetry of [N–I–N]<sup>+</sup> and [N–Br–N]<sup>+</sup> halogen bonding in solution. Preference for a symmetric arrangement was observed for both a freely adjustable and for a conformationally restricted [N–X–N]<sup>+</sup> model system, as also confirmed by computation on the DFT level. A closely attached counterion is shown to be compatible with the preferred symmetric arrangement. The experimental observations and computational predictions reveal a high energetic gain upon formation of symmetric, three-center four-electron halogen bonding. Whereas hydrogen bonds are generally asymmetric in solution and symmetric in the crystalline state, the analogous bromine and iodine centered halogen bonds prefer symmetric arrangement in solution.



## INTRODUCTION

Halogen bonding (XB) refers to the moderately strong, directional, noncovalent interaction of an electropositive halogen (X = Cl, Br, or I) and an electron donating species (D) that can be neutral or anionic in character.<sup>1,2</sup> In the general definition Y–X···D,<sup>1</sup> X is covalently attached to atom Y (Y = C, N, X, etc.) and serves as Lewis acid that accepts electron density from the Lewis base D. The Y–X···D angle is approximately 180°, and the distance between the halogen bonding atoms (X···D) is shorter than the sum of their van der Waals radii. XB interactions were observed first in the 19th century by Guthrie,<sup>3</sup> and were investigated a hundred years later in the solid state by Hassel.<sup>4,5</sup> This phenomenon had been neglected for decades, and has only after its recent rediscovery received immense interest,<sup>6–8</sup> with two decades of studies resulting in applications in a variety of research fields, for example, crystal engineering,<sup>1,9–12</sup> supramolecular chemistry,<sup>13</sup> polymer sciences,<sup>14</sup> liquid crystals,<sup>8,15,16</sup> conductive materials,<sup>9,17,18</sup> and medicinal chemistry.<sup>10–12,19,20</sup> Halogen bonds have so far mostly been studied in the solid and gaseous phases,<sup>30,31</sup> and in silico.<sup>21–25</sup> Lately, the exploration of their applicability in biological systems has started,<sup>11,19,20,26–28</sup> yet so far only a handful of studies of XB have been carried out in solution.<sup>29–36</sup>

The strong resemblance of XB to hydrogen bonding (HB) has been frequently emphasized.<sup>1</sup> As HB is by far the most commonly used secondary interaction for directing molecular recognition processes, reaching an improved understanding of XB is expected to open up exciting opportunities for drug

development, for example. In the assessment of the possible use of HB and XB as complementary molecular tools, understanding their similarities and differences is a prerequisite.

A classic concern regarding HB is its symmetry.<sup>37,38</sup> Originating from its proposed relevance for enzyme catalysis,<sup>39,40</sup> HB symmetry has been studied intensely for decades.<sup>41</sup> Whereas asymmetric in solution ([N–H···N]<sup>+</sup> ⇌ [N···H–N]<sup>+</sup>),<sup>20</sup> hydrogen bonds were shown to be symmetric ([N···H···N]) in crystals.<sup>42,43</sup> In contrast, our understanding of XB symmetry is still in its infancy.<sup>44</sup> Its dependency on the local environment, such as steric and electronic factors, solvent polarity, and the influence of counterions, has not yet been addressed.

Herein, we present an investigation of the symmetry of systems comprised of an electropositive bromine(I) or iodine(I) bound to two nitrogenous electron donors. In such [N···X···N]<sup>+</sup>-type systems, a halogen (X) may either be centered between the two electron donors [N···X···N]<sup>+</sup>, or it may be closer to one of the nitrogens [N–X···N]<sup>+</sup>. The former, symmetric system corresponds to two N···X halogen bonds of equal distance and strength and is characterized by a single-well energy potential (Figure 1a), whereas the second corresponds to a covalent N–X bond and a weaker, longer N···X halogen bond. On the basis of the observations made for closely related HBs,<sup>41</sup> the latter system is expected to exist as a rapidly interconverting mixture of the nonsymmetric tautomers [N–

Received: February 9, 2012

Published: March 5, 2012

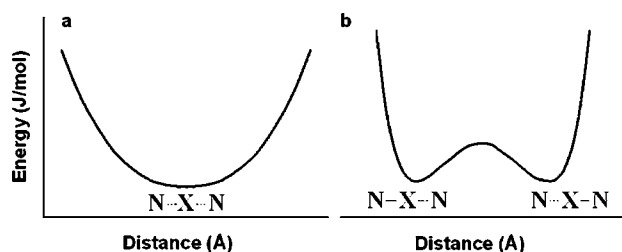


**Figure 1.** Energy potentials for the halogen motion in an N–X–N system: (a) single-well, and (b) double-well. The potential energy variation is shown as a function of the nitrogen–halogen distance. Here, N–X refers to a covalent, N···X to a secondary bond.

X···N<sup>+</sup> and [N···X–N]<sup>+</sup>, which correspond to the two energy minima of a double-well potential (Figure 1b). Originating from the shallow energy barrier between these geometries and the rapidity of the chemical exchange process, most standard spectroscopic methods give coalesced signals for such equilibrating tautomers and are thereby incapable of differentiation between a static symmetric structure, [N···X···N]<sup>+</sup>, and a rapidly equilibrating pair of asymmetric geometries, [N–X···N]<sup>+</sup> ⇌ [N···X–N]<sup>+</sup>. Isotopic substitution causes a slight perturbation of equilibrium processes, but it does not affect static geometries and it can therefore be utilized for differentiation of such systems using NMR spectroscopic detection.<sup>38</sup> Model systems **1a,b** and **2a,b** (Figure 2) comprised

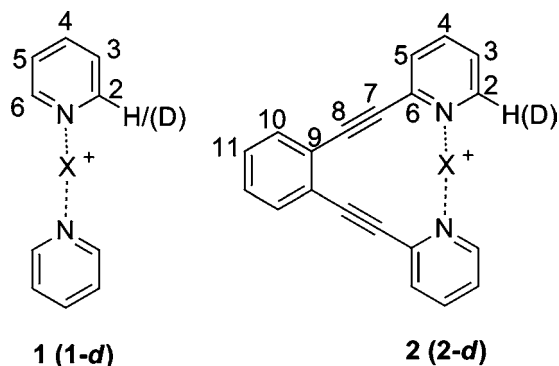


**Figure 2.** Whereas **1** permits free adjustment of N–X distances for most favorable XB or HB interactions, the steric requirements of **2** enforce nonoptimal geometries for a symmetric N–X–N interaction. For **1a** and **2a**, X = Br; for **1b** and **2b**, X = I; for **1c** and **2c**, X = H.

of two pyridine-type Lewis bases binding an electropositive iodine or bromine were studied. They permit linear N–X–N geometry<sup>45,46</sup> necessary for XB,<sup>1</sup> but differ in the ease of availability of N···X distances optimal for two symmetric XB interactions. Importantly, **1a,b** and **2a,b** should not be confused with iodonium or bromonium salts as they consist of a halogen and two pyridines contributing to the N–X bond by a single electron each.<sup>47,48</sup> Hence, the question addressed here is whether the interactions of Br(I) and I(I) to the two coordinating nitrogens are identical, interpretable as two N···X halogen bonds (Figure 1a), or if one of the N–X bonds is stronger than the other, yielding an asymmetric complex having one classical covalent, N–X, and one classical N···X halogen bond (Figure 1b). Whereas **1a,b** may freely adjust to allow for the energetically most favorable interaction, symmetric or asymmetric, the geometrical restriction of the 1,2-diethynylbenzene moiety of **2a,b** offers a slightly longer than

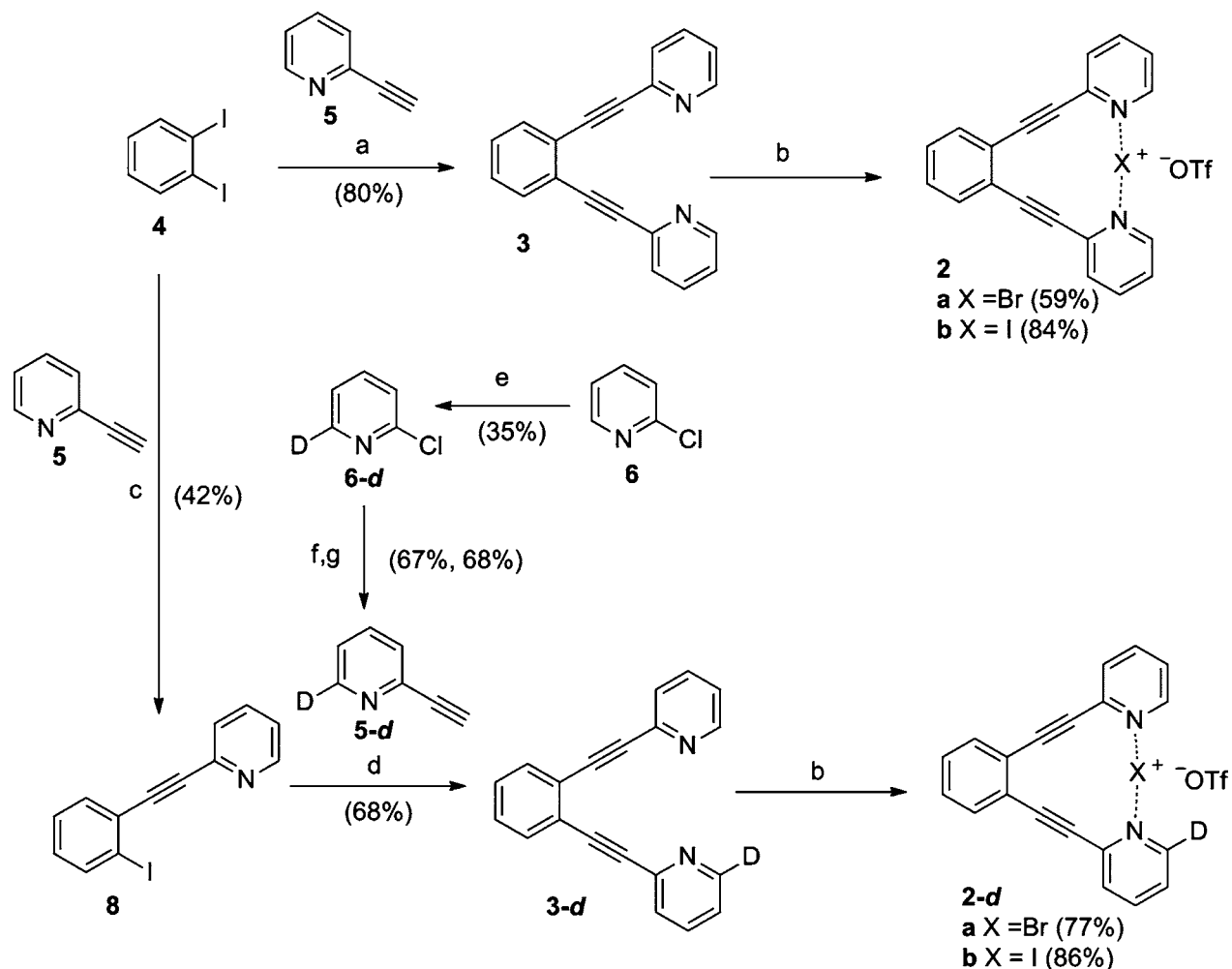
optimal N–N distance for N–X–N interactions, and **2a,b** is thereby expected to possibly promote nonsymmetric geometries. Symmetric complexes of **2** may be achieved by energetically penalized adjustment of its covalent backbone or by alteration of the N–X distances, which in turn prevent optimal orbital overlap. On the other hand, **1a,b** permits an N–X–N axial rotation of the pyridine rings,<sup>44</sup> whereas the aromatic rings of **2a,b** are forced to maintain coplanarity, which may facilitate conjugation of the pyridine  $\pi$ -system to a p-orbital of the coordinating halogen.<sup>48</sup> Here, the investigation of the effect of geometric restraints on halogen bond symmetry is presented. Data for the corresponding bis(pyridinium) triflate HB complexes **1c** and **2c** (Figure 2), which are known to be asymmetric,<sup>38,44</sup> [N–H···N]<sup>+</sup> ⇌ [N···H–N]<sup>+</sup>, are included for comparison.

## RESULTS AND DISCUSSION

For symmetry investigations in solution applying the NMR technique isotopic perturbation of equilibrium (IPE), mixtures of selectively deuterated and nondeuterated compounds are required,<sup>38,49</sup> and were prepared following the procedures summarized below.

**Synthesis.** For the preparation of nondeuterated and deuterated analogues of bis(pyridine)halonium triflates **1a,b** and **1a,b-d** the synthetic protocol of Brown et al. was followed.<sup>50</sup> Pyridine and pyridine-2-*d* in dry dichloromethane were reacted with Br<sub>2</sub> or I<sub>2</sub> in the presence of silver triflate, affording mixtures of [N–Br–N]<sup>+</sup> complexes **1a/1a-d** or [N–I–N]<sup>+</sup> complexes **1b/1b-d** in high yields. Nondeuterated 1,2-bis(2-pyridylethynyl)benzene halonium triflates **2a,b** were synthesized following the route depicted in Scheme 1. Microwave-assisted Sonogashira coupling of diiodobenzene (**4**) and 2 equiv of 2-ethynylpyridine (**5**) afforded compound **3** in high yield.<sup>51</sup> Formation of the [N–X–N]<sup>+</sup> triflate complex with Br<sub>2</sub> or I<sub>2</sub> in the presence of silver triflate provided the bromine(I) and the iodine(I) complexes **2a** and **2b**, respectively, in moderate to high yields.<sup>50</sup> For the generation of the deuterated complexes **2a,b-d**, first regioselective deuteration of 2-chloropyridine (**6**) at C6 was achieved using BuLi–Li–DMAE.<sup>52</sup> Subsequent rapid Sonogashira coupling with TMS-acetylene, followed by KF-mediated deprotection<sup>53</sup> of the alkyne resulted in 6-deutero-2-ethynylpyridine (**5-d**). Sonogashira coupling of **5-d** and **8** furnished **3-d** in moderate yield. The selectively deuterium-labeled [N–X–N]<sup>+</sup> complexes **2a,b-d** were obtained using the conditions given above for **2a,b**.

**NMR Spectroscopic Studies.** Isotopic perturbation of equilibrium (IPE) is a sensitive NMR spectroscopic method that relies on the observation of secondary isotope effects for distinguishing a single symmetric molecule from rapidly interconverting asymmetric tautomers.<sup>49</sup> Its major advantage is that it succeeds even when the rapid exchange causes the NMR signals from the individual tautomers to coalesce into one set of signals, which in turn are virtually identical to those of a single static structure. IPE has been applied successfully, for example, to symmetry determinations of carbocations,<sup>54</sup> O–H···O<sup>55,56</sup> and N–H···N<sup>57,58</sup> HB molecular systems, thiapentenes,<sup>59</sup> and metal chelating complexes.<sup>60</sup> It requires substitution of a proton with deuterium (or, more generally, one isotope with another, e.g., <sup>16</sup>O with <sup>18</sup>O)<sup>61</sup> close to the interaction site, causing changes in the vibration spectrum of the molecule, which eventually affect the observed vibrationally averaged NMR parameters.<sup>62</sup> IPE relies most commonly on <sup>13</sup>C NMR spectroscopic detection and on the analysis of mixtures

Scheme 1. Outline of the Synthesis of **2** and **2-d** (for a, X = Br; for b, X = I)<sup>a</sup>

<sup>a</sup>Reagents and conditions: (a) 2.3 equiv **5**, Pd(PPh<sub>3</sub>)<sub>2</sub>Cl<sub>2</sub>, CuI, Et<sub>2</sub>NH, DMF, MW, 120 °C, 9 min; (b) Br<sub>2</sub> or I<sub>2</sub>, AgOTf, dry CH<sub>2</sub>Cl<sub>2</sub>, rt, N<sub>2</sub> or Ar, 10–15 min; (c) 0.7 equiv **5**, Pd(PPh<sub>3</sub>)<sub>2</sub>Cl<sub>2</sub>, CuI, Et<sub>2</sub>NH, DMF, MW, 120 °C, 4 min; (d) Pd(PPh<sub>3</sub>)<sub>2</sub>Cl<sub>2</sub>, CuI, Et<sub>2</sub>NH, DMF, MW, 120 °C, 13 min; (e) (1) *n*-BuLi, Li-DMAE, dry *n*-hexane, –78 °C, N<sub>2</sub>, 1 h; (2) MeOD, –78 – 0 °C, 30 min; (f) TMS-acetylene, Pd(PPh<sub>3</sub>)<sub>2</sub>Cl<sub>2</sub>, CuI, PPh<sub>3</sub>, Et<sub>2</sub>NH, DMF, MW, 120 °C, 27 min; (g) **7-d**, KF, MeOH, rt, 16 h.

of a nondeuterated molecule and its deuterated analogue. In such a mixture, each observed NMR signal turns into two, one originating from the deuterated molecule and one from the corresponding nondeuterated one, with a small shift difference  ${}^n\Delta_{\text{obs}}$  between them, where  $n$  denotes the number of intervening bonds between the site of the <sup>1</sup>H-to-<sup>2</sup>H substitution and the investigated carbon (eq 1).

$${}^n\Delta_{\text{obs}} = \delta_{\text{C(D)}} - \delta_{\text{C(H)}} \quad (1)$$

The observed shift difference consists of two independent isotope shift contributions: the intrinsic isotope shift  ${}^n\Delta_0$  and the equilibrium isotope shift  ${}^n\Delta_{\text{eq}}$  (eq 2).

$${}^n\Delta_{\text{obs}} = {}^n\Delta_0 + {}^n\Delta_{\text{eq}} \quad (2)$$

In both static and rapidly equilibrating systems, the isotope substitution slightly changes the vibrationally averaged equilibrium geometry and thus causes changes to the intrinsic shift,  ${}^n\Delta_0$ , on all nearby <sup>13</sup>C nuclei. It is usually small (<0.4 ppm) and negative as the <sup>13</sup>C NMR signal corresponding to the heavier, deuterated molecule occurs at a lower chemical shift. The magnitude of  ${}^n\Delta_0$  attenuates rapidly as  $n$  increases. The

second component,  ${}^n\Delta_{\text{eq}}$ , is present only for rapidly tautomerizing systems. Isotope substitution slightly changes the vibrational zero-point energies (ZPE) of the two tautomers, and according to Boltzmann's law, the equilibrium constant  $K$  between the tautomers. This in turn gives a contribution  ${}^n\Delta_{\text{eq}}$  to the isotopic shift that is significant and determined by eq 3:

$${}^n\Delta_{\text{eq}} = D(K - 1)/[2(K + 1)] \quad (3)$$

where  $D$  equals the chemical shift difference between the signals of the tautomeric forms (halogenated N<sup>+</sup>–X and nonhalogenated N, in this particular case). It is noteworthy that sizable  ${}^n\Delta_{\text{eq}}$  need not be restricted to small  $n$ . According to the van't Hoff equation,<sup>63</sup>  $K$  is temperature dependent, and so is therefore  ${}^n\Delta_{\text{eq}}$ . To induce large isotope effects, selective deuterium substitution was performed as close as possible to the [N–X–N]<sup>+</sup> interaction site, at the C2 position of one of the pyridines of **1a–c** and **2a–c** (see Figure 2). Here, the monodeuterated analogues of **1** and **2** are referred to as **1-d** and **2-d**, respectively.

Isotope shifts  ${}^n\Delta_{\text{obs}}$  were obtained by acquisition of <sup>13</sup>C {<sup>1</sup>H, <sup>2</sup>H}NMR spectra of the isotopologues of **1** and **2** dissolved in CD<sub>2</sub>Cl<sub>2</sub>. Similar to previous, related<sup>41</sup> measurements of

intrinsic isotope shifts, mixtures of pyridine and pyridine-2-*d*, and of 1,2-bis(2'-pyridylethynyl)benzene (**3**) and its mono-deuterated analogue **3-d**, respectively, were used as these represent static structures ( ${}^n\Delta_{\text{obs}} = {}^n\Delta_0$ ) most similar to the investigated XB systems **1** and **2**. Isotopic shifts for the halogen bonded complexes and for the static reference systems and the most similar analogous equilibrating systems (N–H–N complexes,<sup>57,58</sup> **1c** and **2c**) are reported in Table 1. Small

**Table 1.** Experimental  ${}^{13}\text{C}$  NMR Isotope Shifts (ppb) at 298 K Measured for  $\text{CD}_2\text{Cl}_2$  Solutions

structure	C2 ${}^1\Delta_{\text{obs}}$	C3 ${}^2\Delta_{\text{obs}}$	C4 ${}^3\Delta_{\text{obs}}$	C5 ${}^4\Delta_{\text{obs}}$	C6 ${}^3\Delta_{\text{obs}}$
Pyridine	−341	−140	0	+14	−15
<b>1a</b>	−307	−139	+17	0	−29
<b>1b</b>	−336	−145	+20	0	−30
<b>1c</b>	−333	−126	+45	+20	−52
<b>2a</b>	−315	−138	+23	0	−25
<b>2b</b>	−334	−145	+24	0	−28
<b>2c</b>	−299	−133	+21	0	−31
<b>3</b>	−333	−135	+13	+15	−17

equilibrium shifts are expected originating from (a) the very small difference in the Lewis basicity of the two nitrogens that is reflected by an equilibrium constant close to unity for the potential tautomerization process  $[\text{N}–\text{X}\cdots\text{N}]^+ \rightleftharpoons [\text{N}\cdots\text{X}–\text{N}]^+$ ,<sup>44</sup> and (b) from the comparably small chemical shift difference (*D*, eq 3) of the halogenated and nonhalogenated, or protonated and nonprotonated (ca. 8 ppm at C2),<sup>64</sup> tautomeric states. Such small equilibrium isotope effects do not permit straightforward, direct differentiation between a static structure and a tautomerizing system.<sup>44</sup> However, the similarity of the observed isotope effects (IEs) at defined positions for the corresponding XB complexes (**1a–2a**, **1b–2b**), for the reference compounds for the static (pyridine, **3**) and the equilibrating systems (**1c**, **2c**) indicate the comparability of the two types of model systems. Originating from their large magnitudes, the  ${}^1\Delta_{\text{obs}}$  and  ${}^2\Delta_{\text{obs}}$  values suffer least from measurement errors, and their comparison among the various compounds is therefore expected to provide the most accurate conclusions. Yet, the magnitude pattern of the 3–4 bond IEs may also be informative. In  $\text{CD}_2\text{Cl}_2$  solutions, comparable  ${}^1\Delta_{\text{obs}}$  and  ${}^2\Delta_{\text{obs}}$  were observed for the static reference compounds pyridine and **3** (Table 1), and for the iodine(I) complexes **1b** and **2b**. The bromine(I) complexes **1a** and **2a** show consequently the lowest IEs, which are comparable to or lower than those observed for the equilibrating references **1c** and **2c**. For distinguishing between a static geometry and the corresponding tautomeric mixture (Figure 1), the temperature dependence of the isotope shifts, expressed as the slopes of  ${}^n\Delta_{\text{obs}}$  versus reciprocal temperature,<sup>65</sup> was studied (Table 2). The small temperature coefficients for the  $\text{CD}_2\text{Cl}_2$  solutions of **1a,b** are indicative of single symmetric structures, whereas the higher coefficients of **1c** confirm its expected asymmetry. In similarity to **1a,b**, the temperature coefficients of the isotope shifts of **2a,b** are comparable and are closer in magnitude to those of the static **3**, than to those of the tautomeric reference **2c**. Thus, IPE analysis indicates single, symmetric structures for **1a,b** and **2a,b** in  $\text{CD}_2\text{Cl}_2$  solution, whereas it confirms the asymmetry for **1c** and **2c**.<sup>57,58</sup>

The observed temperature dependence of the intrinsic isotope effects of the static pyridine and **3** is well-explained by the temperature dependence of solvent polarity.<sup>66</sup> Hence,

**Table 2.** Temperature Coefficients (ppm K) of the Isotope Shifts Reported in Table 1, Observed for  $\text{CD}_2\text{Cl}_2$  Solutions

structure	C2 ${}^1\Delta_{\text{obs}}$	C3 ${}^2\Delta_{\text{obs}}$	C4 ${}^3\Delta_{\text{obs}}$	C5 ${}^4\Delta_{\text{obs}}$	C6 ${}^3\Delta_{\text{obs}}$
Pyridine	−5	−5	0	+2	−3
<b>1a</b>	−3	−6	0	0	−3
<b>1b</b>	−5	−6	1	0	−3
<b>1c</b>	−6	−10	−5	−6	−7
<b>2a</b>	−7	−9	−3	0	−
<b>2b</b>	−7	−7	−2	0	−3
<b>2c</b>	−10	−11	−3	0	+15
<b>3</b>	−5	−7	−3	+2	−2

altered polarity of the environment affects the electron density of the nitrogen lone pair by a dipolar mechanism. Similar through-space polarization by dipolar interaction has been reported previously, for example, for ethers.<sup>67</sup> As the overlap of the nitrogen lone pair with the vicinal C–H/C–D bond has a significant influence on the magnitude of the IE,<sup>68</sup> its temperature dependence indirectly reflects the influence of temperature on the polarity of the environment.

The importance of the local environment on symmetry has been the subject of debates concerned with HB.<sup>37,69</sup> For example, it was proposed that the symmetry of weakly binding charged complexes might be affected by the disorder of the local environment generated by a strongly binding asymmetrically positioned counterion.<sup>69,70</sup> Such an effect is expected to have the strongest influence in nonpolar solvents. To assess the interaction strength of the  $[\text{N}–\text{X}–\text{N}]^+$  XB center with the triflate counterion, translational diffusion coefficients were acquired for  $\text{CD}_2\text{Cl}_2$  solutions of the investigated molecules. Diffusion rates for the  $[\text{N}\cdots\text{X}\cdots\text{N}]^+$  interaction sites were observed by  ${}^1\text{H}$  NMR, and that of triflate anion by  ${}^{19}\text{F}$  NMR. Comparable diffusion coefficients (Table 3) of the correspond-

**Table 3.**  ${}^{15}\text{N}$  NMR Chemical Shifts, and  ${}^1\text{H}$  and  ${}^{19}\text{F}$  NMR Translational Diffusion Coefficients

structure	$\delta({}^{15}\text{N})$ ppm	$D({}^1\text{H}) \times 10^{-10}$ m <sup>2</sup> /s	$D({}^{19}\text{F}) \times 10^{-10}$ m <sup>2</sup> /s
Pyridine	−67.0	30.6	−
<b>1a</b>	−142.9	13.9	14.2
<b>1b</b>	−175.1	14.0	15.0
<b>1c</b>	−134.1	20.3	14.4
<b>2a</b>	−141.2	10.7	10.4
<b>2b</b>	−165.0	10.7	11.7
<b>2c</b>	−137.9	11.7	10.7
<b>3</b>	−64.5	14.5	−

ing positively and negatively charged species indicate tight complexes for each investigated system. Hence, despite strong binding, the triflate ion does not perturb the symmetry of the  $[\text{N}–\text{X}–\text{N}]^+$  XB in apolar  $\text{CD}_2\text{Cl}_2$  solutions. This fact is explained either by a symmetric arrangement of the triflate, with equal distances to the pyridine nitrogens, or by a close, asymmetric orientation of the counterion, which is incapable of breaking the strongly stabilized symmetric  $[\text{N}\cdots\text{X}\cdots\text{N}]^+$  halogen bond. The generally higher diffusion rates of the bipyridyl complexes, **1a–c**, as compared to the 1,2-bis(2'-pyridylethynyl)benzene complexes, **2a–c**, originate from their smaller size, that is, smaller solvent accessible surface area.

Strong interaction with the counterion without loss of symmetry suggests a significant energetic gain upon formation of the static, symmetric 3-center-4-electron XB,<sup>48,71</sup> which



observation is in excellent agreement with the previously reported exceptionally high strength of analogous halogen and hydrogen bonds, for example,  $[I-I \cdots I]^-$  and  $[F-H \cdots F]^-$  of 160–180 kJ/mol.<sup>1,72</sup>

As a sensitive indicator for the changes of the nitrogen bond order and electron density,<sup>73</sup> the <sup>15</sup>N chemical shifts were measured for free pyridine and for compounds **1**–**3** using <sup>1</sup>H,<sup>15</sup>N-HMBC experiments.<sup>74,75</sup> For each compound, a single nitrogen signal was detected (Table 3).

Upon complexation, alteration of the nitrogen chemical shift was observed for **1**–**2**, but to a different extent for the protonated (pyridine–**1c**, –67 ppm) and the bromine (pyridine–**1a**, –76 ppm) and iodine centered (pyridine–**1b**, –108 ppm) halogen bonded systems (Table 3). A larger chemical shift change may be interpretable as a stronger interaction and may imply an increasing covalent character in the order H < Br < I. The <sup>15</sup>N chemical shift change upon formation of the bromine centered halogen bond of **1a** is similar to that upon protonation (**1c**, Table 3), whereas the iodine centered XB of **1b** caused a <sup>15</sup>N chemical shift alteration comparable to the shift change caused by N-alkylation (N-methylpyridinium iodide,  $\delta_{N15} = -180.5$  ppm). This latter observation may be rationalized in several ways. (a) It may be a result of stabilization of the  $[N-I-N]^+$  interaction by  $\sigma$ -overlap of an empty iodine p-orbital and the filled nonbonding orbital of the nitrogens simultaneously with an efficient overlap of a filled p-orbital of I(I) and the nitrogen  $\pi^*$ -orbitals, which are involved in the aromatic system of the complexing pyridines.<sup>48</sup> Electron donation from the pyridine  $\pi$ -orbitals to the bromine or iodine d-orbitals may also contribute. This explanation is supported by the coplanarity of bis(pyridine)halonium complexes in crystals.<sup>46,48,50</sup> (b) It may be due to an exceptionally strong electrostatic  $N^{\delta-} \cdots I^+$  interaction; however, in light of the noncomparable smaller  $\Delta\delta_N$  upon protonation of pyridine, this explanation appears less likely. (c) A large chemical shift change may also be rationalized as indication of a stronger halogen bond by resonance stabilization<sup>41</sup> or (d) by an increased covalent character.<sup>76</sup> Geometry optimization, discussed in detail below, predicts  $d_{N-I} = 2.3$  Å for **2b**, which is close to the sum of the covalent radii of N and I (2.1 Å) and significantly shorter than the sum of their van der Waals radii (3.5 Å). The ca. 10 ppm higher <sup>15</sup>N shift of **2b** compared to **1b** may reflect its weaker N–I bonds, interpretable here as the consequence of the steric restraint introduced by the diethynylbenzene backbone that strives for longer than optimal N–N distance for the symmetric  $[N \cdots I \cdots N]^+$  complex. Notably, the XB symmetry of **2b** is retained. The <sup>15</sup>N chemical shift changes of **1a** and **2a** reveal comparable, yet weaker interactions. A less favorable interaction of the bromine(I) complex **2a** compared to **1a** is further indicated by its apparently lower stability in solutions.

**Computation.** For theoretical confirmation of the experimental results, the equilibrium geometries and energies of **1a**–**c**,<sup>44</sup> **2a**–**c** and **3** were calculated using density functional theory (DFT), employing the B3LYP exchange and correlation functional.<sup>77–80</sup> The LANL08 basis set<sup>81</sup> in conjunction with the LANL2DZ effective core potential<sup>82–84</sup> were used for Br and I, Pople's 6-311++G(d,p) basis set<sup>85–87</sup> for N and the central H atoms in **2c** and **3c**, and Pople's 6-311G(d,p) basis set<sup>86,87</sup> for the remaining atoms. Solvent effects were accounted for by the Polarizable Continuum Model (PCM),<sup>88,89</sup> with CH<sub>2</sub>Cl<sub>2</sub> as solvent.<sup>44</sup> All calculations were done with the Gaussian09 program package.<sup>90</sup> The delocalized electrons in

the 3-center-4-electron bonds make a DFT description of **1a**–**c** and **2a**–**c** challenging, owing on the one hand to the incomplete description of nondynamic electron correlation in these bonds,<sup>91</sup> and on the other to the self-interaction error inherent to DFT.<sup>92</sup> However, reference calculations<sup>44</sup> with second-order Møller–Plesset perturbation theory (MP2)<sup>93</sup> for **1a**–**c** confirm that DFT provides a reasonable description of these complexes.

Table 4 shows computed N–X and N–N bond distances for **1a,b** and **2a,b**, along with reference distances calculated for

**Table 4.** Computationally Predicted N–X and N–N Distances [Å] for the Equilibrium Geometries of **1a**–**c**, **2a**–**c**, and **3**<sup>a</sup>

Structure	X	$d_{N-X(1)}$	$d_{N-X(2)}$	$d_{N-N}$
	H	1.015	-	-
	Br	1.890	-	-
	I	2.092	-	-
	H	1.069	1.733	2.802
	Br	<i>1.291</i>	<i>1.291</i>	<i>2.582</i>
	Br	2.139	2.139	4.278
	I	2.301	2.301	4.602
	H	1.082	1.648	2.730
	Br	<i>1.287</i>	<i>1.287</i>	<i>2.574</i>
	I	2.140	2.140	4.280
	I	2.302	2.302	4.604
	H	1.049	1.911	2.935
	Br	<i>1.316</i>	<i>1.316</i>	<i>2.619</i>
	I	2.140	2.140	4.280
	I	2.303	2.303	4.602
	-	-	-	4.680

<sup>a</sup>Calculations were done at the B3LYP level with the basis set and ECPs described in the computational section, employing PCM with CD<sub>2</sub>Cl<sub>2</sub> as solvent. Values in italics refer to unstable symmetric structures. Those for **1a**–**c** are taken from reference 44.

protonated (**1c**, **2c**) and halogenated pyridine as well as for **3**. DFT calculations predict symmetric geometries for **1a,b** and **2a,b** (Figure 3, Supporting Information) and asymmetric ones for **1c** and **2c**, confirming the experimental findings. The N–Br and N–I bond distances in **1a,b** and **2a,b** are less than 0.3 Å longer than their counterparts in the hypothetical brominated or iodinated pyridine, which indicates that the N–X bonds in **1a,b** and **2a,b** show a significant covalent character. For the stable asymmetric structures of **1c** and **2c**, the elongation of the shorter N–H bond compared to protonated pyridine is less than 0.07 Å, and thus closely resembles that in protonated pyridine. A longer N–N distance was predicted for **3** (4.68 Å) than for the complexes **1a** (4.28 Å), **1b** (4.60 Å), and, most notably, **1c** (2.58 and 2.80 Å for the symmetric and asymmetric structure, respectively). As a consequence of the strain provided by the backbone of **3**, longer N–X distances and lower stability for **2a**–**c** as compared to **1a**–**c** are expected. This conjecture is only partially confirmed by computation (Table 4). The largest difference between the complexes of the freely adjustable **1** and of the rigidified **2** is predicted for the protonated complex. For

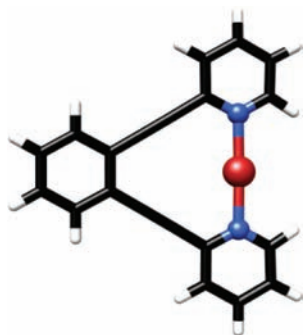


**Figure 3.** DFT geometry optimization (DFT, B3LYP LANL08) predicts a static, symmetric  $[N\cdots X\cdots N]^+$  **2a** complex with  $d_{N-Br} = 2.1$  Å. This distance is between the sum of the covalent (1.9 Å) and the sum of the van der Waals radii (3.4 Å) of N and Br. Optimized structures of **2b** and **2c** are shown in the Supporting Information.

the stable asymmetric structure, the longer N–H bond is elongated by 0.35 Å in **2c** as compared to **1c**, and the N–N distance increases by 0.2 Å. For the symmetric structure of **2c**, the N–H distance increases by 0.03 Å, and the N–N distance adjusts by 0.045 Å. It should further be noted that, in **2c**, the N–H–N bonds become bent with a bond angle of 165°.

For **2a** and **2b**, the increase in the N–X and N–N distances as compared to **1a** and **1b** is below 0.001 Å. These findings suggest that **3**, in spite of its conjugated covalent nature, is easily distorted. This proposal is supported by the X-ray crystallographic studies of related substances.<sup>94–96</sup> The equilibrium geometry of **3** is influenced by Coulomb repulsion between the lone pairs of the nitrogen atoms, which repulsion is neutralized upon complexation of a cation in **2a–c**. The strain introduced by rearrangement of **3** from its equilibrium geometry to the geometries found in **2a,b** is slightly negative (ca.  $-2$  kJ mol<sup>-1</sup>). Remarkably, the comparably large geometric rearrangement of **3** for forming **2c** yields an estimated strain energy of only 6 kJ mol<sup>-1</sup> (for a detailed discussion of the strain energies see Supporting Information). Consequently, the N–X–N three-centered bond of **2a,b** shows comparable geometries to those of **1a,b** with the primary difference that a coplanar geometry is enforced for the pyridine rings of **2a,b**, whereas free rotation around the N–X–N axis is allowed for the pyridines of **1a,b**.

Informative measures for the stability of the studied complexes are provided by the computed frequencies of their N–X stretching vibrations (Table 5) and their estimated relative stabilities (Table 6). The signature of the asymmetric N–X–N stretching vibrations is consistent with symmetric **1a,b** and **2a,b** and asymmetric **1c** and **2c**. Comparable vibrational frequencies, with less than 10 cm<sup>-1</sup> difference, were predicted for the Br and I complexes (Table 5). As a general trend, all frequencies of **2a,b** are approximately 20 cm<sup>-1</sup> (symmetric) to 30 cm<sup>-1</sup> (antisymmetric vibration modes) lower than their counterparts in **1a,b**. However, this difference does not necessarily indicate a lower stability of **2a,b** as compared to **1a,b**, but may rather be the consequence of the larger reduced masses for **2a,b**. For **1c** and **2c**, the N–H and N⋯H stretching vibrations show markedly different frequencies (ratio >20), reflecting the large difference in their bond strengths. This difference is more distinct for **2c** than for **1c**, in line with the calculated bond length alternations discussed above. The estimated relative stabilities of the complexes **1a–c**, shown in Table 6, indicate higher binding energies for the

**Table 5.** Computed Frequencies [cm<sup>-1</sup>] for the N–X and N–N Stretching Vibrations for **1a–c**, **2a–c**, and **3**<sup>a</sup>

Structure	X	$\nu_{\text{symm}}^b$	$\nu_{\text{asymm}}^c$
	-	3570.3 <sup>d</sup>	-
	Br	317.1 <sup>d</sup>	-
	I	260.1 <sup>d</sup>	-
<b>1c</b>	H	2601.7 <sup>d</sup>	143.1 <sup>e</sup>
		<i>241.0</i>	<i>i1052.3</i>
<b>1a</b>	Br	172.5	162.6
	I	167.0	166.8
<b>1b</b>	H	2374.3 <sup>d</sup>	124.4 <sup>e</sup>
		<i>216.0</i>	<i>i996.0</i>
<b>1a</b>	Br	172.8	162.4
	I	167.1	166.4
<b>2c</b>	H	2952.0 <sup>d</sup>	99.8 <sup>e</sup>
		<i>214.5</i>	<i>i1313.3</i>
<b>2a</b>	Br	158.0	135.2
	I	148.9	137.9
<b>2b</b>	H	24.7	
<b>3</b>	H	24.7	

<sup>a</sup>Calculations done at B3LYP level with the basis set and ECPs described in the computational section, employing PCM with CD<sub>2</sub>Cl<sub>2</sub> as solvent. Values in italics refer to unstable symmetric structures. Values for **1a–c** are taken from the literature.<sup>44</sup> <sup>b</sup>Symmetric N–X–N stretching vibration unless otherwise stated. <sup>c</sup>Antisymmetric N–X–N stretching vibration unless otherwise stated. <sup>d</sup>N–X stretching vibration. <sup>e</sup>N⋯X stretching vibration.

halogen(I) as compared to the protonated complex (difference 60–70 kJ mol<sup>-1</sup>). It should be noted that the bond energies of **1a,b** and **2a,b** are comparable in magnitude to that of a covalent bond. The difference between protonated and halogenated complexes may be partly ascribed to the higher stability of HOTf compared to BrOTf and IOTf. The computed bond energies of **2a–c** ( $\Delta E$ ) are approximately 20 kJ mol<sup>-1</sup> weaker than their counterparts in **1a–c**. At first glance, this result might be ascribed to the reorganization energy of **3**. However, this energy is close to zero for the formation of **2a,b** and about 6 kJ mol<sup>-1</sup> for the formation of **2c**, as shown above. Also, the observed energy difference is nearly constant from **2a** to **2c**, whereas the reorganization energy increases from **2a** to **2c**. Thus, the different formation energies are likely to originate from electronic effects, for example, from differences in the degree of delocalization of the  $\pi$ -systems in the complexes of **1** versus **2**. The  $\Delta G$  values are equal (**c**) or slightly larger (**a,b**) for **2** as compared to **1**, reflecting a smaller entropy loss upon formation of **2a,c** than of **1a,c**, depending on the number of entities associating throughout complexation.

A comparison of the energies for planar and twisted conformers of **1a–c** (Table 6) confirm the hypothesis that the pyridine rings of **1a,b** freely rotate around the N–X–N axis. For **1c**, the twisted conformation appears to be favored; however, this prediction should not be overly trusted since an incorrect treatment of the hindered rotation around the N–X–N axis as soft vibration cannot be ruled out,<sup>97</sup> and hence, the entropy balance between the planar and the twisted forms may be described incorrectly.

Table 6. Predicted Stabilities [ $\text{kJ mol}^{-1}$ ] of **1a–c** and **2a–c**<sup>a</sup>

Structure	Reference	X	$\Delta E$	$\Delta G$
		H	-64.0	-53.5
		Br	-89.2	-79.7
		I	-60.1	-51.5
	2	H <sup>b</sup>	-113.8	-68.2
		Br	-180.2	-121.9
		I	-167.6	-103.1
		H <sup>b</sup>	-92.5	-68.4
		Br	-161.8	-123.0
		I	-144.9	-113.0
		H	4.3	7.6
		Br	0.2	0.0
		I	0.1	0.1
		H	6.4	4.6
		Br	0.2	0.0
		I	0.1	0.1
		H	22.3	7.5
		Br	0.2	0.0
		I	0.1	0.1

<sup>a</sup>Calculations were done at B3LYP level of theory with the basis set and ECPs described in the computational section, employing the PCM with  $\text{CD}_2\text{Cl}_2$  as solvent.  $\Delta E$  denotes the electronic energy, and  $\Delta G$  the Gibbs free energy at 298 K. Values for **1a–c** are taken from reference 44. Underlined values are potentially flawed by the improper treatment of a hindered rotation, such as soft vibration in the entropy term.<sup>97</sup>  
<sup>b</sup>Refers to the asymmetric structure.

The inversion barrier for **2c** is  $16 \text{ kJ mol}^{-1}$  higher in energy than that for **1c** (Table 6), in agreement with the fact that the steric strain in **3** hinders inversion (the N–N distance is shorter in the symmetric form of **2c** than in the asymmetric one). However, ZPE and entropy effects largely equalize this difference between **1c** and **2c**. Further computational confirmation for the symmetric XB geometries of **2a,b** were provided by relaxed potential energy surface (PES) calculations at the B3LYP/LACVP\* level using  $\text{CH}_2\text{Cl}_2$  continuum solvent model, as implemented in Jaguar (Schrödinger, Inc.), and scanned for geometries with varying N–X distances in 0.05 Å steps. The PES scans predict a single energy minimum with  $d_{\text{N–Br}} = 2.19 \text{ Å}$  for **2a** and  $d_{\text{N–I}} = 2.30 \text{ Å}$  for **2b**, in contrast with a double well potential for **2c** with optimal  $d_{\text{N–H}}$  distances of 1.05 Å and 1.96 Å.

## CONCLUSIONS

Combined NMR spectroscopic and computational investigation indicates the strong preference for the static, symmetric arrangement of bromine and iodine centered  $[\text{N}\cdots\text{X}\cdots\text{N}]^+$ -type XB in solutions. Translational diffusion measurements revealed a tight interaction of the positively charged halogen bonded complex with the triflate counterion. Such close interactions were previously concluded to be responsible for asymmetries observed in crystals; however, they do not cause any observable destabilization of the symmetric arrangements of **1a,b** and **2a,b** in  $\text{CH}_2\text{Cl}_2$  solutions. Interestingly, related  $[\text{N–Br–N}]^+$  systems

are often asymmetric,<sup>44,50,98</sup> whereas  $[\text{N–I–N}]^+$  are symmetric<sup>99</sup> in the solid state. In contrast,  $[\text{N–H–N}]$  hydrogen bonds are asymmetric in solution and symmetric in crystals.<sup>38</sup> This fact reveals that despite the often emphasized similarities of HB and XB,<sup>1</sup> there are distinct differences as well that may become of vast importance in the development of XB to a complementary molecular tool to HB in rational drug design strategies. The higher stability of the symmetric arrangement of 3-center-4-electron halogen bonds compared to hydrogen bonds in solutions may originate from a more efficient overlap of the nitrogen lone pairs with the p-orbital<sup>48</sup> of  $\text{I}^+$  or  $\text{Br}^+$  as compared to the possible overlap with the empty s orbital of  $\text{H}^+$ . The advantageous orbital overlap yields a covalent character for the investigated XB systems, revealed by <sup>15</sup>N chemical shift data analysis as well as by computation. Experimental findings were supported by DFT analysis predicting symmetric  $[\text{N}\cdots\text{X}\cdots\text{N}]^+$  arrangements for **1a,b** and **2a,b**.

An important aspect of this work is that the systems studied provide simple models for the investigation of 3-center-4-electron halogen bonds. A well-known example for such a halogen bonded complex is the  $\text{I}_3^-$  ion, which has been the target of intense debate in the halogen bonding community.<sup>100,101</sup> The triiodide ion was previously reported both to be symmetric ( $d_{\text{I–I}} = 2.90 \text{ Å}$ )<sup>102,103</sup> and asymmetric ( $d_{\text{I–I}} = 2.83$  and  $3.03 \text{ Å}$ )<sup>46,104–106</sup> in the solid state, depending on its environment. It is often cited as the strongest halogen bonded complex ( $180 \text{ kJ mol}^{-1}$ ).<sup>1</sup> The suggestion of the exceptional halogen bond donor strength of  $\text{X}^{\delta+}$  is further confirmed by this investigation. Related trihalide ions, such as  $\text{Br}_3^-$ ,  $\text{I}_2\text{Br}^-$ , and  $\text{IBr}_2^-$ , were typically found to be asymmetric in crystals.<sup>104</sup> The assessment of the symmetry of trihalide ions in solutions is considerably more difficult than the investigation of the related model compounds **1** and **2**, and could therefore so far only be predicted by computation.<sup>107–111</sup>

A further impact of the present investigation is that  $[\text{N–X–N}]^+$  complexes are common reagents used in electrophilic halogenations.<sup>50,112–121</sup> Gaining an improved understanding of the structure of such halogenation agents, for example, of the Barluenga's reagent,<sup>113–115</sup> is therefore of relevance in synthetic organic chemistry. In these reactions,  $\text{X}^+$  is transferred from an  $[\text{N–X–N}]^+$  bond to a  $\text{C}=\text{C}$  double bond through a  $[\text{C–X–C}]^+$  intermediate. Whereas the symmetry of the  $[\text{C–X–C}]^+$  intermediate has been extensively studied,<sup>122–124</sup> the symmetry of the halonium transfer reagent has so far received little attention.<sup>44,125,126</sup>

The presented NMR and computational study of **1c** agrees well with the previous conclusions on hydrogen bond asymmetry based on computational (DFT),<sup>127</sup> solution<sup>37,38</sup> and solid state<sup>127</sup> NMR spectroscopic investigations. However, the proposal of a general asymmetry of HB in solutions has been questioned by the Limbach group, who based on solution and solid state NMR studies argued that HB symmetry depends on the local environment (counterion, neighboring molecules), and that strong hydrogen bonds may be symmetric or exhibit only small deviations from symmetry.<sup>70,128–130</sup> Moreover, for hydrogen bonds exhibiting tautomeric behavior, they proposed that isotopic perturbation observed by NMR may not originate from equilibrium isotope effects caused by zero point energy changes, but from equilibrium averaged intrinsic or geometric isotope effects arising from anharmonic ground state vibrations.<sup>131</sup> It should be noted that recent UV–vis spectroscopic studies of Limbach<sup>129</sup> support the findings of



Perrin.<sup>56</sup> The conclusion of hydrogen bond asymmetry based on IPE studies has recently been further criticized by Singleton et al.,<sup>132</sup> who by computational methods, yet ignoring the related computational work of Ohta,<sup>123</sup> proposed that IPE data attributed to isotopic perturbation of equilibria may in certain cases be better interpreted as the consequence of isotope induced desymmetrization of symmetrical potential energy surfaces. Spectroscopic observation (IPE) and computational (DFT) prediction of symmetric geometries for **1a,b** and **2a,b** whereas of asymmetric ones for the closely related **1c** and **2c** do not support this proposal. Furthermore, the magnitude of the <sup>2h</sup>J<sub>NN</sub> scalar coupling determined through the N–H···N intermolecular hydrogen bond (10.2 ± 0.4 Hz) of bis-(pyridinium) tetrachlorogallate [(Py–H···Py)(GaCl<sub>4</sub>)],<sup>127</sup> closely related to compound **1c**, by solid state NMR best fits to an asymmetric arrangement (*d*<sub>N1–N2</sub> = 2.707 Å, *d*<sub>N1–H</sub> = 0.946 Å, *d*<sub>N2–H</sub> = 1.761 Å). This observation agrees well with the asymmetric geometry of **1c** (Table 4). The X-ray crystallographic analysis of bis(2-methylpyridinium) tetraphenylborate revealed an electron density pattern best compatible with a single, symmetric, strongly hydrogen bonded geometry; yet the possibility that the N–H–N hydrogen would occupy a double well rather than a single well potential in crystal could not be excluded.<sup>99</sup> This may be rationalized by (a) the inhibition of dynamic characteristics in crystals,<sup>127</sup> or by an inherent weakness of X-ray crystallography (b) to recognize dynamic processes and (c) to accurately refine hydrogen positions.<sup>133</sup> The alternative views on hydrogen bond symmetry indicate that the analysis of weakly binding complexes remains a challenge. Unequivocal determination of HB and XB symmetry necessitates the careful, simultaneous use of alternative spectroscopic and computational methods.

## ■ ASSOCIATED CONTENT

### Ⓢ Supporting Information

Details on the synthesis depicted in Scheme 1, spectroscopic data for compound identification, and details on the NMR and computational symmetry investigations. This material is available free of charge via the Internet at <http://pubs.acs.org>.

## ■ AUTHOR INFORMATION

### Corresponding Author

mate@chem.gu.se

### Present Addresses

<sup>||</sup>Department of Chemistry, University of Bergen, NO-5020 Bergen, Norway.

<sup>§</sup>AstraZeneca R&D Mölndal, Medicinal Chemistry, S-431 83 Mölndal, Sweden.

### Notes

The authors declare no competing financial interest.

## ■ ACKNOWLEDGMENTS

We are grateful to Alexei A. Neverov (Department of Chemistry, Queen's University, Canada) for helpful advice regarding the synthesis of halonium complexes,<sup>50</sup> and to Charles L. Perrin (Department of Chemistry and Biochemistry, University of California San Diego, CA) for instructive discussions. We thank Per-Ola Norrby (Department of Chemistry and Molecular Biology, University of Gothenburg) for valuable advice regarding the relaxed scan calculations. The research leading to these results has received funding from the European Union Seventh Framework Programme (FP7/2007-

2013) under grant agreement no. 259638. We thank the Swedish Research Council (2007:4407; 621-2008-3562) and the Carl Tryggers Foundation for financial support.

## ■ REFERENCES

- (1) Metrangolo, P.; Neukirch, H.; Pilati, T.; Resnati, G. *Acc. Chem. Res.* **2005**, *38*, 386.
- (2) Politzer, P.; Lane, P.; Concha, M. C.; Ma, Y.; Murray, J. S. *J. Mol. Model.* **2007**, *13*, 305.
- (3) Guthrie, F. *J. Chem. Soc.* **1863**, *16*, 239.
- (4) Hassel, O.; Hvoslef, J. *Acta Chem. Scand.* **1954**, *8*, 873.
- (5) Hassel, O. *Science* **1970**, *170*, 497.
- (6) Metrangolo, P.; Meyer, F.; Pilati, T.; Resnati, G.; Terraneo, G. *Angew. Chem., Int. Ed.* **2008**, *47*, 6114.
- (7) Cavallo, G.; Metrangolo, P.; Pilati, T.; Resnati, G.; Sansotera, M.; Terraneo, G. *Chem. Soc. Rev.* **2010**, *39*, 3772.
- (8) Roper, L. C.; Prasang, C.; Kozhevnikov, V. N.; Whitwood, A. C.; Karadakov, P. B.; Bruce, D. W. *Cryst. Growth Des.* **2010**, *10*, 3710.
- (9) Fourmigue, M.; Auban-Senzier, P. *Inorg. Chem.* **2008**, *47*, 9979.
- (10) Bissantz, C.; Kuhn, B.; Stahl, M. *J. Med. Chem.* **2010**, *53*, 5061.
- (11) Lu, Y.; Shi, T.; Wang, Y.; Yang, H.; Yan, X.; Luo, X.; Jiang, H.; Zhu, W. *J. Med. Chem.* **2009**, *52*, 2854.
- (12) Parisini, E.; Metrangolo, P.; Pilati, T.; Resnati, G.; Terraneo, G. *Chem. Soc. Rev.* **2011**, *40*, 2267.
- (13) Resnati, G.; Metrangolo, P. *Chem.—Eur. J.* **2001**, *7*, 2511.
- (14) Metrangolo, P.; Resnati, G.; Pilati, T.; Liantonio, R.; Meyer, F. *J. Polym. Sci., Part A; Polym. Chem.* **2007**, *45*, 1.
- (15) Bruce, D. W.; Metrangolo, P.; Meyer, F.; Prasang, C.; Resnati, G.; Terraneo, G.; Whitwood, A. C. *New J. Chem.* **2008**, *32*, 477.
- (16) Bruce, D. W.; Metrangolo, P.; Meyer, F.; Pilati, T.; Prasang, C.; Resnati, G.; Terraneo, G.; Wainwright, S. G.; Whitwood, A. C. *Chemistry* **2010**, *16*, 9511.
- (17) Fourmigue, M.; Batail, P. *Chem. Rev.* **2004**, *104*, 5379.
- (18) Brezgunova, M.; Shin, K. S.; Auban-Senzier, P.; Jeannin, O.; Fourmigue, M. *Chem. Commun.* **2010**, *46*, 3926.
- (19) Lu, Y. X.; Wang, Y.; Zhu, W. L. *Phys. Chem. Chem. Phys.* **2010**, *12*, 4543.
- (20) Hardegger, L. A.; Kuhn, B.; Spinnler, B.; Anselm, L.; Ecabert, R.; Stihle, M.; Gsell, B.; Thoma, R.; Diez, J.; Benz, J.; Plancher, J. M.; Hartmann, G.; Banner, D. W.; Haap, W.; Diederich, F. *Angew. Chem., Int. Ed.* **2011**, *50*, 314.
- (21) Clark, T.; Hennemann, M.; Murray, J. S.; Politzer, P. *J. Mol. Model.* **2007**, *13*, 291.
- (22) Politzer, P.; Murray, J. S.; Clark, T. *Phys. Chem. Chem. Phys.* **2010**, *12*, 7748.
- (23) Riley, K. E.; Hobza, P. *J. Phys. Chem. B* **2008**, *112*, 3157.
- (24) Tawarada, R.; Seio, K.; Sekine, M. *J. Org. Chem.* **2008**, *73*, 383.
- (25) Eskandari, K.; Zariny, H. *Chem. Phys. Lett.* **2010**, *492*, 9.
- (26) Auffinger, P.; Hays, F. A.; Westhof, E.; Ho, P. S. *Proc. Natl. Acad. Sci. U.S.A.* **2004**, *101*, 16789.
- (27) Voth, A. R.; Hays, F. A.; Ho, P. S. *Proc. Natl. Acad. Sci. U.S.A.* **2007**, *104*, 6188.
- (28) Voth, A. R.; Khoo, P.; Oishi, K.; Ho, P. S. *Nat. Chem.* **2009**, *1*, 74.
- (29) Metrangolo, P.; Panzeri, W.; Recupero, F.; Resnati, G. *J. Fluorine Chem.* **2002**, *114*, 27.
- (30) Mele, A.; Metrangolo, P.; Neukirch, H.; Pilati, T.; Resnati, G. *J. Am. Chem. Soc.* **2005**, *127*, 14972.
- (31) Sarwar, M. G.; Dragisic, B.; Sagoo, S.; Taylor, M. S. *Angew. Chem., Int. Ed.* **2010**, *49*, 1674.
- (32) Dimitrijevic, E.; Kvak, O.; Taylor, M. S. *Chem. Commun.* **2010**, *46*, 9025.
- (33) Sarwar, M. G.; Dragisic, B.; Salsberg, L. J.; Gouliaras, C.; Taylor, M. S. *J. Am. Chem. Soc.* **2010**, *132*, 1646.
- (34) Serpell, C. J.; Kilah, N. L.; Costa, P. J.; Felix, V.; Beer, P. D. *Angew. Chem., Int. Ed.* **2010**, *49*, 5322.
- (35) Bruckmann, A.; Pena, M. A.; Bolm, C. *Synlett* **2008**, 900.
- (36) Erdelyi, M. *Chem Soc Rev* **2012**. DOI: 10.1039/C2CS15292D.



- (37) Perrin, C. L. *Science* **1994**, *266*, 1665.
- (38) Perrin, C. L. *Pure Appl. Chem.* **2009**, *81*, 571.
- (39) Gerlt, J. A.; Kreevoy, M. M.; Cleland, W.; Frey, P. A. *Chem. Biol.* **1997**, *4*, 259.
- (40) Cleland, W. W.; Kreevoy, M. M. *Science* **1994**, *264*, 1887.
- (41) Perrin, C. L. *Acc. Chem. Res.* **2010**, *43*, 1550.
- (42) Borisov, E. V.; Skorodumov, E. V.; Pachevskaya, V. M.; Hansen, P. E. *Magn. Reson. Chem.* **2005**, *43*, 992.
- (43) Ellison, R. D.; Levy, H. A. *Acta Crystallogr.* **1965**, *19*, 260.
- (44) Carlsson, A. C. C.; Gräfenstein, J.; Laurila, J. L.; Bergquist, J.; Erdelyi, M. *Chem. Commun.* **2012**, *17*, 1458.
- (45) Schuster, I. L.; Roberts, J. D. *J. Org. Chem.* **1979**, *44*, 2658.
- (46) Hassel, O.; Hope, H. *Acta Chem. Scand.* **1961**, *15*, 407.
- (47) Lin, G. H. Y.; Hope, H. *Acta Crystallogr., Sect. B: Struct. Sci.* **1972**, *B 28*, 643.
- (48) Alcock, N. W.; Robertson, G. B. *J. Chem. Soc. Dalton Trans.* **1975**, 2483.
- (49) Siehl, H. U. *Adv. Phys. Org. Chem.* **1987**, *23*, 63.
- (50) Neverov, A. A.; Feng, H. X.; Hamilton, K.; Brown, R. S. *J. Org. Chem.* **2003**, *68*, 3802.
- (51) Erdelyi, M.; Gogoll, A. *J. Org. Chem.* **2001**, *66*, 4165.
- (52) Gros, P.; Choppin, S.; Mathieu, J.; Fort, Y. *J. Org. Chem.* **2002**, *67*, 234.
- (53) Erdelyi, M.; Langer, V.; Karlen, A.; Gogoll, A. *New J. Chem.* **2002**, *26*, 834.
- (54) Saunders, M.; Telkowski, L.; Kates, M. R. *J. Am. Chem. Soc.* **1977**, *99*, 8070.
- (55) Perrin, C. L.; Lau, J. S.; Kim, Y. J.; Karri, P.; Moore, C.; Rheingold, A. L. *J. Am. Chem. Soc.* **2009**, *131*, 13548.
- (56) Perrin, C. L.; Lau, J. S. *J. Am. Chem. Soc.* **2006**, *128*, 11820.
- (57) Perrin, C. L.; Ohta, B. K. *J. Am. Chem. Soc.* **2001**, *123*, 6520.
- (58) Perrin, C. L.; Ohta, B. K. *Bioorg. Chem.* **2002**, *30*, 3.
- (59) Perrin, C. L.; Kim, Y. J.; Kuperman, J. *J. Phys. Chem. A* **2001**, *105*, 11383.
- (60) Perrin, C. L.; Kim, Y. J. *Inorg. Chem.* **2000**, *39*, 3902.
- (61) Perrin, C. L.; Karri, P. *Chem. Commun.* **2010**, *46*, 481.
- (62) Perrin, C. L.; Flach, A. *Angew. Chem., Int. Ed.* **2011**, *50*, 7674.
- (63) van't Hoff, J. H. Z. *Phys. Chem.* **1887**, *1*, 483.
- (64) Perrin, C. L.; Karri, P. *J. Am. Chem. Soc.* **2010**, *132*, 12145.
- (65) Perrin, C. L.; Kim, Y. J. *J. Am. Chem. Soc.* **1998**, *120*, 12641.
- (66) Strauss, C. R.; Trainor, R. W. *Aust. J. Chem.* **1995**, *48*, 1665.
- (67) Perrin, C. L.; Erdelyi, M. *J. Am. Chem. Soc.* **2005**, *127*, 6168.
- (68) Perrin, C. L.; Ohta, B. K.; Kuperman, J.; Liberman, J.; Erdelyi, M. *J. Am. Chem. Soc.* **2005**, *127*, 9641.
- (69) Perrin, C. L. *Acc. Chem. Res.* **2010**, *43*, 1550.
- (70) Pietrzak, M.; Wehling, J. P.; Kong, S.; Tolstoy, P. M.; Shenderovich, I. G.; Lopez, C.; Claramunt, R. M.; Elguero, J.; Denisov, G. S.; Limbach, H. H. *Chemistry* **2010**, *16*, 1679.
- (71) Hope, H.; Lin, G. H. Y. *Chem. Commun.* **1970**, 169.
- (72) Emsley, J. *Chem. Soc. Rev.* **1980**, *9*, 91.
- (73) Duthaler, R. O.; Roberts, J. D. *J. Am. Chem. Soc.* **1978**, *100*, 4969.
- (74) Meier, S.; Benie, A. J.; Duus, J. O.; Sorensen, O. W. *ChemPhysChem* **2009**, *10*, 893.
- (75) Parella, T. *Magn. Reson. Chem.* **1998**, *36*, 467.
- (76) Chen, J. G.; McAllister, M. A.; Lee, J. K.; Houk, K. N. *J. Org. Chem.* **1998**, *63*, 4611.
- (77) Becke, A. D. *J. Chem. Phys.* **1993**, *98*, 5648.
- (78) Lee, C.; Yang, W.; Parr, R. G. *Phys. Rev. B: Condens. Matter* **1988**, *37*, 785.
- (79) Vosko, S. H.; Wilk, L.; Nusair, M. *Can. J. Phys.* **1980**, *58*, 1200.
- (80) Stephens, P. J.; Devlin, F. J.; Chabalowski, C. F.; Frisch, M. J. *J. Phys. Chem.* **1994**, *98*, 11623.
- (81) Roy, L. E.; Hay, P. J.; Martin, R. L. *J. Chem. Theory Comput.* **2008**, *4*, 1029.
- (82) Hay, P. J.; Wadt, W. R. *J. Chem. Phys.* **1985**, *82*, 270.
- (83) Wadt, W. R.; Hay, P. J. *J. Chem. Phys.* **1985**, *82*, 284.
- (84) Hay, P. J.; Wadt, W. R. *J. Chem. Phys.* **1985**, *82*, 299.
- (85) Clark, T.; Chandrasekhar, J.; Spitznagel, G. W.; Schleyer, P. v. R. *J. Comput. Chem.* **1983**, *4*, 294.
- (86) Francl, M. M.; Pietro, W. J.; Hehre, W. J.; Binkley, J. S.; Gordon, M. S.; Defrees, D. J.; Pople, J. A. *J. Chem. Phys.* **1982**, *77*, 3654.
- (87) Raghavachari, K.; Binkley, J. S.; Seeger, R.; Pople, J. A. *J. Chem. Phys.* **1980**, *72*, 650.
- (88) Mennucci, B.; Tomasi, J. *J. Chem. Phys.* **1997**, *106*, 5151.
- (89) Cossi, M.; Scalmani, G.; Rega, N.; Barone, V. *J. Chem. Phys.* **2002**, *117*, 43.
- (90) Frisch, M. J.; Trucks, G. W.; Schlegel, H. B.; Scuseria, G. E.; Robb, M. A.; Cheeseman, J. R.; Scalmani, G.; Barone, V.; Mennucci, B.; Petersson, G. A.; Nakatsuji, H.; Caricato, M.; Li, X.; Hratchian, H. P.; Izmaylov, A. F.; Bloino, J.; Zheng, G.; Sonnenberg, J. L.; Hada, M.; Ehara, M.; Toyota, K.; Fukuda, R.; Hasegawa, J.; Ishida, M.; Nakajima, T.; Honda, Y.; Kitao, O.; Nakai, H.; Vreven, T.; Montgomery, J., J. A.; Peralta, J. E.; Ogliaro, F.; Bearpark, M.; Heyd, J. J.; Brothers, E.; Kudin, K. N.; Staroverov, V. N.; Kobayashi, R.; Normand, J.; Raghavachari, K.; Rendell, A.; Burant, J. C.; Iyengar, S. S.; Tomasi, J.; Cossi, M.; Rega, N.; Millam, N. J.; Klene, M.; Knox, J. E.; Cross, J. B.; Bakken, V.; Adamo, C.; Jaramillo, J.; Gomperts, R.; Stratmann, R. E.; Yazyev, O.; Austin, A. J.; Cammi, R.; Pomelli, C.; Ochterski, J. W.; Martin, R. L.; Morokuma, K.; Zakrzewski, V. G.; Voth, G. A.; Salvador, P.; Dannenberg, J. J.; Dapprich, S.; Daniels, A. D.; Farkas, Ö.; Foresman, J. B.; Ortiz, J. V.; Cioslowski, J.; Fox, D. J. *Gaussian09*; Gaussian, Inc.: Wallingford, CT, 2010.
- (91) Becke, A. D. *J. Chem. Phys.* **2003**, *119*, 2972.
- (92) Grafenstein, J.; Cremer, D. *Theor. Chem. Acc.* **2009**, *123*, 171.
- (93) Möller, C.; Plesset, M. S. *Phys. Rev.* **1934**, *46*, 0618.
- (94) Wandell, H.; Wiest, O. *J. Org. Chem.* **2002**, *67*, 388.
- (95) Baldwin, K. P.; Matzger, A. J.; Scheiman, D. A.; Tessier, C. A.; Vollhardt, K. P. C.; Youngs, W. J. *Synlett* **1995**, 1215.
- (96) Yamakawa, J.; Ohkoshi, M.; Takahashi, F.; Nishiuchi, T.; Kuwatani, Y.; Nishinaga, T.; Yoshida, M.; Iyoda, M. *Chem. Lett.* **2008**, *37*, 784.
- (97) Ayala, P. Y.; Schlegel, H. B. *J. Chem. Phys.* **1998**, *108*, 2314.
- (98) Blair, L. K.; Parris, K. D.; Hii, P. S.; Brock, C. P. *J. Am. Chem. Soc.* **1983**, *105*, 3649.
- (99) Glidewell, C.; Holden, H. D. *Acta Crystallogr., B* **1982**, *38*, 667.
- (100) In *Categorizing Halogen Bonding and Other Noncovalent Interactions Involving Halogen Atoms*, IUCr 2011 Satellite Workshop: Sigüenza, Spain, 2011.
- (101) Abate, A.; Brischetto, M.; Cavallo, G.; Lahtinen, M.; Metrangolo, P.; Pilati, T.; Radice, S.; Resnati, G.; Rissanen, K.; Terraneo, G. *Chem Commun* **2010**, *46*, 2724.
- (102) Slater, R. C. L. *Acta Crystallogr.* **1959**, *12*, 187.
- (103) Bent, H. A. *Chem. Rev.* **1968**, *68*, 587.
- (104) Davies, J. E.; Nunn, E. K. *Chem. Commun.* **1969**, 1374.
- (105) Mooney, R. C. L. Z. *Kristallogr.* **1935**, *90*, 143.
- (106) Tasman, H. A.; Boswijk, K. H. *Acta Crystallogr.* **1955**, *8*, 59.
- (107) Zhang, F. S.; Lynden-Bell, R. M. *Phys. Rev. Lett.* **2003**, *90*.
- (108) Zhang, F. S.; Lynden-Bell, R. M. *Eur. Phys. J. D* **2005**, *34*, 129.
- (109) Margulis, C. J.; Coker, D. F.; Lynden-Bell, R. M. *Chem. Phys. Lett.* **2001**, *341*, 557.
- (110) Margulis, C. J.; Coker, D. F.; Lynden-Bell, R. M. *J. Chem. Phys.* **2001**, *114*, 367.
- (111) Sato, H.; Hirata, F.; Myers, A. B. *J. Phys. Chem. A* **1998**, *102*, 2065.
- (112) Arsequell, G.; Espuna, G.; Valencia, G.; Barluenga, J.; Carlon, R. P.; Gonzalez, J. M. *Tetrahedron Lett.* **1999**, *40*, 7279.
- (113) Barluenga, J. *Pure Appl. Chem.* **1999**, *71*, 431.
- (114) Barluenga, J.; Rodriguez, M. A.; Campos, P. J. *J. Org. Chem.* **1990**, *55*, 3104.
- (115) Barluenga, J.; Rodriguez, M. A.; Gonzalez, J. M.; Campos, P. J. *Tetrahedron Lett.* **1990**, *31*, 4207.
- (116) Barluenga, J.; Rodriguez, M. A.; Campos, P. J. *Tetrahedron Lett.* **1990**, *31*, 2751.
- (117) Barluenga, J.; Campos, P. J.; Lopez, F.; Llorente, I.; Rodriguez, M. A. *Tetrahedron Lett.* **1990**, *31*, 7375.

- (118) Barluenga, J.; Gonzalez-Bobes, F.; Murguia, M. C.; Ananthoju, S. R.; Gonzalez, J. M. *Chemistry* **2004**, *10*, 4206.
- (119) Lopez, J. C.; Bernal-Albert, P.; Uriel, C.; Valverde, S.; Gomez, A. M. *J. Org. Chem.* **2007**, *72*, 10268.
- (120) Huang, K. T.; Winssinger, N. *Eur. J. Org. Chem.* **2007**, 1887.
- (121) Barluenga, J.; Gonzalez, J. M.; Garciamartin, M. A.; Campos, P. *J. Tetrahedron Lett.* **1993**, *34*, 3893.
- (122) Ohta, B. K.; Hough, R. E.; Schubert, J. W. *Org. Lett.* **2007**, *9*, 2317.
- (123) Ohta, B. K.; Scupp, T. M.; Dudley, T. J. *J. Org. Chem.* **2008**, *73*, 7052.
- (124) Olah, G. A.; Bollinger, J.; Brinich, J. *J. Am. Chem. Soc.* **1968**, *90*, 2587.
- (125) Sabin, J. R. *J. Mol. Struct.* **1971**, *7*, 407.
- (126) Haque, I.; Wood, J. L. *J. Mol. Struct.* **1968**, *2*, 217.
- (127) Claramunt, R. M.; Perez-Torrallba, M.; Maria, D. S.; Sanz, D.; Elena, B.; Alkorta, I.; Elguero, J. *J. Magn. Reson.* **2010**, *206*, 274.
- (128) Benedict, H.; Limbach, H. H.; Wehlan, M.; Fehlhammer, W. P.; Golubev, N. S.; Janoschek, R. *J. Am. Chem. Soc.* **1998**, *120*, 2939.
- (129) Koeppe, B.; Tolstoy, P. M.; Limbach, H. H. *J. Am. Chem. Soc.* **2011**, *133*, 7897.
- (130) Lesnichin, S. B.; Tolstoy, P. M.; Limbach, H. H.; Shenderovich, I. G. *Phys. Chem. Chem. Phys.* **2010**, *12*, 10373.
- (131) Sharif, S.; Denisov, G. S.; Toney, M. D.; Limbach, H. H. *J. Am. Chem. Soc.* **2006**, *128*, 3375.
- (132) Bogle, X. S.; Singleton, D. A. *J. Am. Chem. Soc.* **2011**, *133*, 17172.
- (133) Almlöf, J.; Ottersen, T. *Acta Crystallogr., A* **1979**, *35*, 137.